Available online at www.sciencedirect.com
SCIENCE DIRECT®
ELSEVIER
Nuclear Instruments and Methods in Physics Research B 226 (2004) 153–162
NIM B
Beam Interactions with Materials & Atoms
www.elsevier.com/locate/nimb

Silver surface enrichment of silver–copper alloys: a limitation for the analysis of ancient silver coins by surface techniques

L. Beck [a,*], S. Bosonnet [a], S. Réveillon [a], D. Eliot [a], F. Pilon [b]

[a] *Unité d'enseignement de physique et étude des matériaux, INSTN, CEA Saclay, 91191 Gif-sur-Yvette Cedex, France*
[b] *Laboratoire d'expertises chimiques et physico-chimiques, Dept. Matériaux, CEA Le Ripault, BP16, 37260 Monts, France*

Received 21 October 2003; received in revised form 15 June 2004

Abstract

The surface enrichment of archaeological silver–copper alloys has been recognized for many years. However, the origin of this enrichment is not well defined and many hypotheses have been put forward to account for this behaviour: segregation of the components during casting, deliberate thermal and/or chemical post-treatment, abrasion or corrosion. Among the hypotheses mentioned above, we have focused our study on the first step of coin manufacturing. Replications of silver–copper standards of various compositions ranging from 30% to 80% Ag, reflecting the composition of silver blanks, have been produced. Metallographic examination, PIXE and SEM–EDS have been used for the characterization of each sample. A model of the direct enrichment has been established. This model allows us to propose a relationship between the surface composition and the silver content of the core. Comparison with data of Roman coins from the Roman site of Châteaubleau (France) and from the literature and consequences for the analyses of ancient coins by surface methods are presented.

PACS: 81.05.Bx; 82.80.Ej; 07.85.Tt
Keywords: X-ray spectrometry; PIXE; SEM–EDS; Silver–copper alloys; Debased silver; Silver enrichment; Roman silver coins; Châteaubleau

1. Introduction

In numismatics, the determination of the original alloy composition is important to know the genuine fineness of the coins. The relative proportion of major elements provides valuable information

* Corresponding author. Tel.: +33 1 6908 4871; fax: +33 1 6908 3869.
E-mail address: lucile.beck@cea.fr (L. Beck).

0168-583X/$ - see front matter © 2004 Elsevier B.V. All rights reserved.
doi:10.1016/j.nimb.2004.06.044

on changes in monetary theory, economic changes and materials technology. Such studies require the analysis of a large number of coins in order to follow the evolution of coinage over the centuries. Consequently, non-destructive techniques are preferred.

A pioneer study was made by Walker in the mid-1970s [1]. He analyzed more than 5000 silver coins by X-ray fluorescence (XRF). King and Northover more recently used electron-probe microanalysis (EPMA) to study silver coins of the third century AD [2]. XRF is widespread in laboratories due to its ease of use, and outside of laboratories because of the availability of portable systems [3]. At the beginning of the 1980s, particle induced X-ray emission (PIXE) was applied to archaeological samples and to the analysis of ancient coins. A review of PIXE and XRF for the analysis of archaeological metals is presented in [4]. Well known for its low limits of detection, PIXE therefore requires the use of an ion accelerator. XRF, EPMA and PIXE are recognized as surface methods since only a surface layer of limited depth (from a few micrometers up to a few tens of micrometers) is analyzed. By contrast, fast neutron activation analysis (FNAA) offers the most advantageous means of obtaining access to the bulk composition [5,6]. This technique, as well as proton activation analysis (PAA) [7,8] which is semi-global, have been successfully applied to the study of numerous coinages [9]. [1]

In case of noble metals, surface enrichment for gold or silver alloys has been reported by several authors [10,11]. In order to obtain reliable analyses, Walker [1], as well as King and Northover [2] have abraded the coins to remove the Ag-enriched layers and then mainly analyzed the core of the coins by EPMA. Basutçu [12] has used various analytical methods for the analysis of Ag in Ag–Cu coins. A comparison of PAA with FNAA indicates that surface enrichment can be up to 20% compared to the composition of the core. Additional results from particle-induced gamma-ray emission (PIGE) at 3 MeV with helium (penetration depth approximately up to 3 μm) or with protons (penetration depth approximately up to 20 μm) give information on the strength of the surface enrichment within the first micrometers. Brissaud et al. [13] have compared FNAA, PIXE and XRF results of Gaulish silver coins and noticed a marked overestimation of silver content by these surface techniques. Weber et al. [14] have studied the heterogeneity of silver ingots by comparison of PIXE analyses on etched and non-etched surfaces. The authors have remarked that the accuracy of the fineness is restored after removing approximately 10 μm of the superficial layer. Klockenkämper et al. [15] have studied in detail the near-surface silver enrichment of 218 Roman Imperial coins at two different investigation depths (3 and 30 μm) by means of EPMA–EDS and XRF–WDS. The comparison of their results with Walker's data allows them to estimate the extent of the surface enrichment. In a recent paper, Linke et al. [16] have observed an important enrichment of the surface of medieval silver coins by comparing EDXRF and PIXE measurements on the surface of the coins and microanalysis on the cross-sections by scanning electron microscopy with energy dispersive spectrometry (SEM–EDS). Differences up to 50% between the composition of the core and the surface have been obtained.

In most of the papers mentioned above, many hypotheses have been proposed to explain the silver surface enrichment of silver–copper alloys: (a) segregation during casting or annealing [10,14,17], (b) deliberate thermal and/or chemical post-treatment such as pickling in acids [10,11] or blanching [18–20], (c) wearing [21] and (d) corrosion [10,12,16,18,22,23]. This list should also include post-excavation cleaning with diluted acids (e.g. H_2SO_4) in order to identify and classify the coins, which can also affect the surface composition.

The aim of this work is to make an attempt to identify the main cause of the surface enrichment of silver–copper alloys. Among the hypotheses mentioned above, we have focused our study on the first step of coin manufacturing. Silver–copper standards of various compositions, reflecting the composition of silver blanks, have been produced. Metallographic examination, PIXE and SEM–

[1] Several examples are published in Les Cahiers Ernest-Babelon, J.-N. Barrandon (Dir.), CNRS Editions, Paris.

EDS have been used for the characterization of each sample. The same experiments have been carried out on five Roman coins. Three other Roman coins were only analyzed by non-destructive techniques.

From the results of this set of samples, a model of enrichment can be proposed and a relationship regarding the surface composition as a function of the bulk silver content is suggested.

2. Sample preparation and investigation techniques

Each replication was prepared from pure silver and copper in following bulk compositions: 80/20 (Rep. A); 72/28 (Rep. B); 50/50 (Rep. C); 30/70 (Rep. D) – % Ag/% Cu. The weight of each sample was about 3.7 g, similar to that of the coins under study. The metals were placed in a cold crucible (mix of clay and graphite) and melted in the furnace at 1200 °C for 15 min. Samples were left in the furnace during cooling. Both processes were done in air. Each button was sectioned in two parts and both pieces were mounted in epoxy resin. The samples were polished on their surfaces and partially etched with HNO_3 and H_2O_2. Investigations were carried out by optical microscope, magnification 50–1000 (Leica MF 4M) and by SEM–EDS (Cambridge S120) with Si(Li) detector. Analyses were also performed by PIXE (2 MeV protons, beam diameter: 100 or 200 μm, 2.5 MeV Van de Graaff accelerator and Si(Li) detector).

For comparison, a set of Roman silver coins was also included in this survey (Table 1). Five coins (nos. 1–5), which could be sectioned were observed by metallographic examination and analyzed by SEM–EDS and PIXE on both surface and cross-section. These coins were recently found at the excavation site of Châteaubleau (Seine-et-Marne, France) [24]. This Gallo-Roman site, located at the via Agrippa (trade route between Boulogne-sur-Mer, Lyon and Milan) was an important agglomeration from the first to the fourth century AD. Two other coins (nos. 6 and 7) from a private collection could not be damaged and were therefore analyzed non-destructively by PIXE and FNAA (CNRS Orléans, France). Coin no. 8 is a counterfeit coin consisting of a copper blank covered by a silver–copper alloy [25]. The surface layer was analyzed by PIXE on the surface and by SEM–EDS on the cross-section.

3. Results

3.1. Replication

Two microstructures of Ag–Cu alloys are presented in Fig. 1(a) (Rep. A: 80% Ag/20% Cu) and 1(b) (Rep. D: 30% Ag/70% Cu). When cooling, the Ag–Cu alloys undergo phase separation. The core microstructure of each replication is in agreement with the expected structure: for Rep. A, the primary phase consists of a silver-rich phase (Ag > 91.2%), while for Rep. D, the primary phase is copper-rich (Cu > 92%). In both samples, the grains (or dendrites) are surrounded by the eutectic phase (72% Ag). Microanalysis of the grains gives results which in composition correspond very

Table 1
Description of the coins and summary of the analytical techniques used

Coin no.	Date (AD)	Emperor	Denomination/Type or reference	Analytical techniques
1	147–149	Antoninus	Denarius RIC III, 168–183	SEM–EDS surface/cross-section
2	193–196	Septimius Severus	Denarius RIC IV-1, 538	SEM–EDS and PIXE surface/cross-section
3	249–250	Trajan Decius	Antoninianus RIC IV-3, 16c	SEM–EDS and PIXE surface/cross-section
4	253–254	Gallienus	Antoninianus RIC V-1, 132	SEM–EDS and PIXE surface/cross-section
5	261	Gallienus	Antoninianus RIC V-1, 317	SEM–EDS and PIXE surface/cross-section
6	262	Postumus	Antoninianus E. 299/Cun 2395	PIXE surface FNAA bulk
7	268	Postumus	Antoninianus E. 565/Cun 2450	PIXE surface FNAA bulk
8	≈262–268	Postumus	Antoninianus forgery	PIXE surface SEM–EDS cross-section

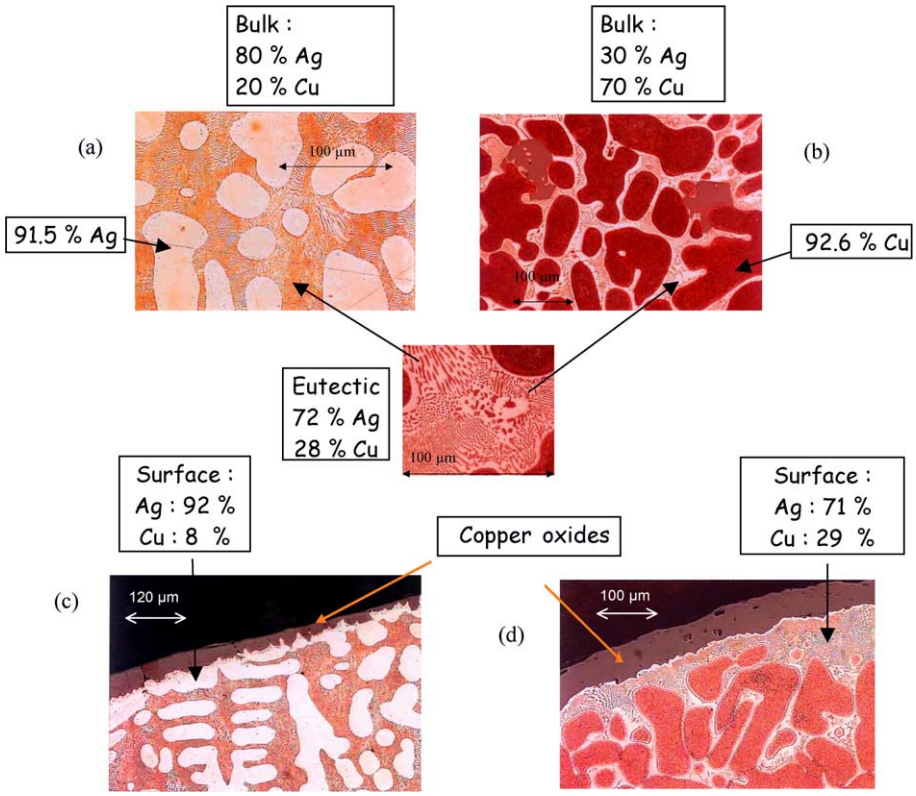

Fig. 1. Microstructure of two silver–copper alloys. (a) and (c): core and surface of an 80%Ag–20%Cu alloy. (b) and (d): core and surface of a 30%Ag–70%Cu alloy.

well to the solid formed from the melt in the phase diagram for Ag–Cu.

In contrast, two different behaviours of the components can be observed at the surface according to the sample. For Rep. A, silver-rich grains accumulate at the surface (Fig. 1(c)). The grains are connected and then form a continuous layer along the external part of the sample. The composition of the grains is 91.5% Ag and the thickness of this layer ranges from 20 to 80 μm. For Rep. D, the sample is covered by a continuous and regular layer of the eutectic phase (Fig. 1(d)). SEM–EDS gives an Ag concentration of 70.9%, close to the theoretical values (72% Ag). The thickness of this layer ranges from 10 to 40 μm. This layer is connected with the eutectic network of the core. Rep. C presents the same feature. The structure of Rep. B consists of the eutectic mix. On the top of each replication, a layer of copper oxides is observed.

Except Rep. B, all samples show a heterogeneous microstructure. In addition to the expected dendrite formation, segregation at the surface of the alloys could be observed. Normal segregation is responsible for the large concentration of the silver-rich phase (Ag > 92%) at the surface of silver-rich alloys (Ag > 72%). Inverse segregation is observed for alloys with an Ag concentration below 72% with the formation of a eutectic layer (Ag = 72%) at the surface. Summing up, an enriched layer is observed at the surface of the samples, depending on the initial bulk composition (Table 2).

Table 2
Surface and bulk compositions of the Ag–Cu replications

	Bulk	Surface
Hypereutectoic alloy	Ag > 72%	Ag ⩾ 92%
Hypoeutectoic alloy	30 < Ag < 72%	Ag = 72%

Table 3
Surface and bulk composition of eight Roman coins

Coin no.		Ag (%)			Cu (%)			Pb (%)		
		SEM–EDS	PIXE	FNAA	SEM–EDS	PIXE	FNAA	SEM–EDS	PIXE	FNAA
1	Surface	99			1					
	Bulk	92			7			1		
2	Surface	98	96		2	3			1	
	Bulk	74	77		21	22		1		
3	Surface[a]	95	93		3	5		1	2	
	Bulk	36	33		63	62		1	1	
4	Surface	71	72		20	21		2	3	
	Bulk	23	20		74	78		1	1	
5	Surface	–[b]	7		–[b]	59		–[b]	9	
	Bulk	3	3		90	88		3	4	
6	Surface		26			72			1	
	Bulk			14.6			84.6			0.4
7	Surface		36			58			3	
	Bulk			12.5			86.0			0.9
8	Surface		78			11			1	
	Bulk	26			66			1		

"Surface" refers to the surface composition. The probe (proton or electron) is perpendicular to the coin surface and the depth penetration is a few microns. "Bulk" refers to the global composition obtained either by the analysis on the cross-section of the coins (PIXE and SEM–EDS) or by global analysis (FNAA).

[a] Coin cleaned with H_2SO_4 during field-work.

[b] Surface too deteriorated to be analyzed by SEM–EDS.

3.2. Coins

The concentration in Ag, Cu and Pb of the eight coins analyzed are summarized in Table 3. Other elements such as Sn, Au and Fe have been detected in trace element level, but are not reported in the table. Six coins (nos. 1–5 and 8) were observed by metallographic examination and analyzed by SEM–EDS and/or PIXE. Results from both techniques are in good agreement with allowance for some area size effects and the heterogeneity of the samples (proton beam spot area: ≈8 or 3×10^{-2} mm^2; electron scanning area: ≈2–6×10^{-3} mm^2).

Comparison between surface and bulk composition clearly show a strong surface enrichment within the first microns. Coins 1 and 2 show a surface silver content greater than 96% for bulk silver

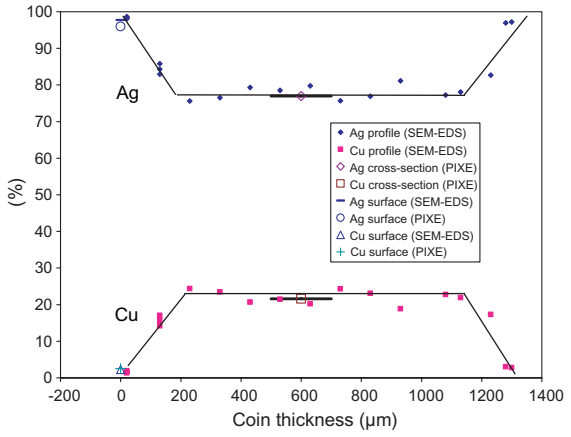

Fig. 2. Ag and Cu profiles along the depth of coin no. 2. Each point represents the analysis of a 40 μm × 60 μm area.

contents of 74% and 92%. Silver and copper profiles along the depth of coin no. 2 are shown in Fig. 2. Coin 3 was cleaned with H_2SO_4 during field-work; this acid pickling seems to enhance the Ag surface content (more than 92% for a bulk composition of about 35%). Coins 4 and 8 have 72% and 78% Ag at the surface, whereas the bulk compositions are respectively 20% and 26%. Coins 5–7 show various surface compositions, all below 36% Ag.

4. Discussion

4.1. Surface enrichment of the silver–copper replications

The surface composition as a function of the initial composition of the replications is shown in Fig. 3. Three main regions (a, c and d) can be distinguished, separated on one side by the eutectic composition ($Ag_{bulk} = 72\%$) and on the another side by $Ag_{bulk} \simeq 18\%$. Work is in progress to determine this limit with more precision.

In order to explain these three different behaviours, a representation of the surface enrichment of the silver–copper alloys can be proposed (Fig. 4). The structures depend on the initial composition of the alloys. For silver–copper alloys with more than 72% Ag (Fig. 4(a)), the surface composition follows the composition of the silver-rich primary phase (Ag = 92%), i.e. in equilibrium conditions, the composition given by the phase diagram. For silver–copper alloys with less than 72% Ag, the surface composition has the eutectic composition (Ag = 72%, Fig. 4(c)) until the continuity

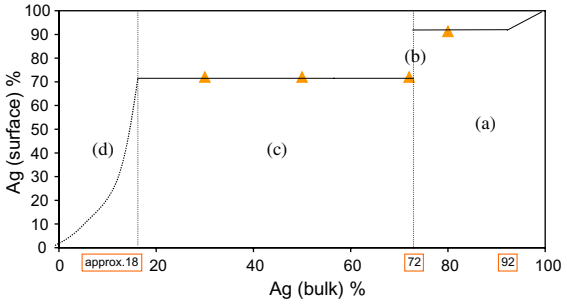

Fig. 3. Surface Ag content of the replications as a function of the bulk Ag content. Labels (a)–(d) refer to Fig. 4.

of the eutectic layer is preserved (Fig. 4(d)). At very low Ag content (Ag < 15–20%), the silver proportion seems to be too low for forming a continuous eutectic layer. In that case, the resultant surface layer is seen to be thin and/or porous (Fig. 4(d)) and the surface composition is the mean between the eutectic and copper-rich phases. The abrupt change at $Ag_{bulk} = 72\%$ not only corresponds to the changes in the core microstructure, but also to the changes in the surface structure.

The enrichment phenomenon of debased silver alloys has been described by Cope as a consequence of the heating of the coins during fabrication and particularly during the preparation of the coins from buttons and blanks, in the intermediate stages of the conventional Roman minting practice [10]. He proposed a mode of formation of a silver surface on copper–debased silver coinage alloy by five successive steps (Fig. 5(a)): (1) casting button of silver–copper alloy, (2) heating the button in air to form a layer of copper oxides, (3) acid-pickling the flan for removing the copper oxides and revealing the silver-phase, (4) hammering the blank for spreading silver-phase laterally and (5) striking the blank.

In the case of the replications, the elevated-temperature oxidation phenomena occurred in the early stage of the sample fabrication and has resulted in the formation of a continuous layer of the silver-rich phase at the surface of the button (Fig. 5(b)). The surface enrichment is then directly achieved and it was not necessary to proceed with the other steps ((2) and (4)), except the removal of the copper oxide. The results show the ability to obtain a directly enriched silver layer on silver–copper alloy containing more than 15–20% Ag. For lower Ag contents, the method proposed by Cope is still well suited, since the structure (Fig. 4(d)) is similar to that described in his article (reproduced here in Fig. 5(a), step (1)). For other compositions, the method proposed by Cope remains correct if no direct oxidation is achieved.

4.2. Comparison between the replications and the coins

For comparison, the model described above (Fig. 3) and the results observed at the coins are

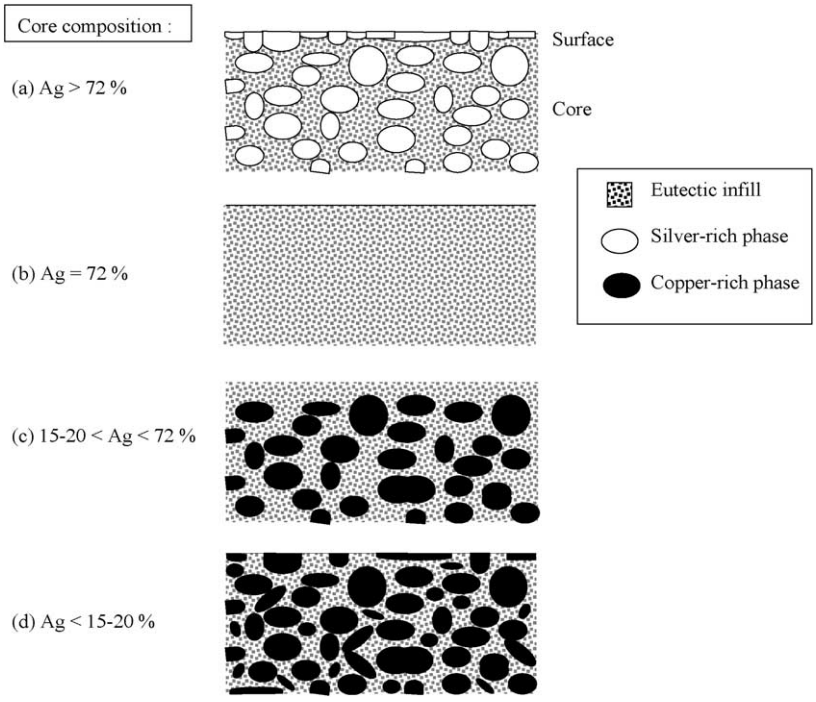

Fig. 4. Schematic representation of silver–copper alloy surfaces.

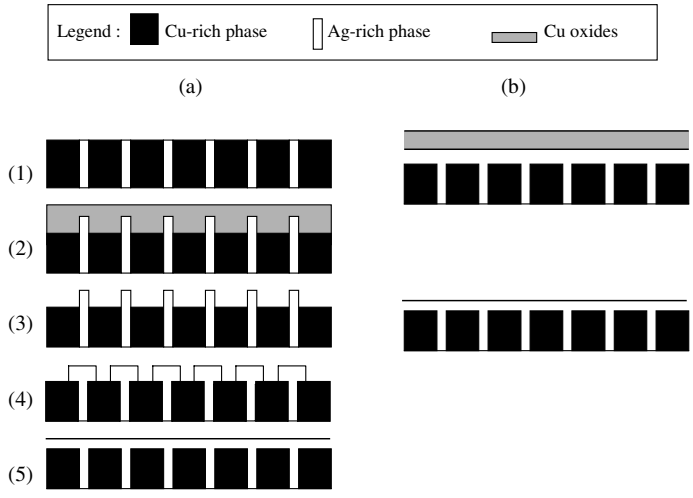

Fig. 5. Comparison of (a) the schematic representation of the surface enrichment proposed by Cope [10] and (b) the direct enrichment observed for the replications.

plotted in Fig. 6. Data from literature are also included (Table 4). Globally, the results of the coins follow the model proposed. The model described in this study only takes into account processes

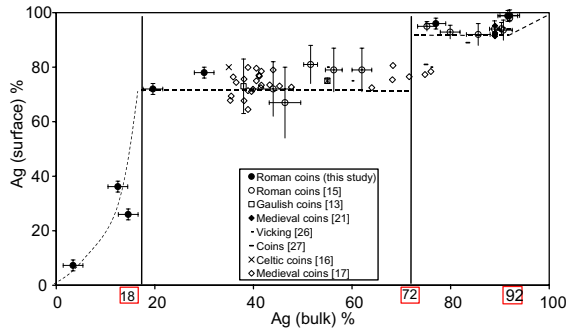

Fig. 6. Surface composition as a function of the core composition of silver–copper coins. Techniques used for data acquisition presented in this figure are described in Table 4. For our analyses, error bars represent an estimation of the absolute uncertainty: ±2%. For data of reference [15], circles represent the mean of the analyses by emperor and error bars the standard deviation (1σ).

occurring during the first steps of the fabrication of the coins. The good agreement between the model and the analysis results suggests that the enrichment process of the coins mainly arises from the stage of the blank fabrication. We have shown that this stage is characterized by a segregation of the silver-rich phases towards the external part of the sample and is responsible for the significant silver surface enrichment ($71 < Ag_{surf} < 99\%$) of the alloys ($20 < Ag_{bulk} < 92\%$).

Apart from the fabrication process, it has been considered that silver enrichment of the silver–copper alloys could also be caused by further stages such as additional annealing, blanching or corrosion [16,18,20]. During the corrosion process or the chemical treatments, copper could be leached, letting appear on the surface of the coins the structures richest in silver. For alloys with $20\% < Ag_{bulk} < 72\%$, the richest silver phase is the eutectic phase which contains 72% Ag. As a consequence, these phenomena, occurring after fabrication of the coins, may produce or reinforce surface enrichment close in composition to that obtained by the direct process described in this study. The data provided by Linke et al. [16], also given in Fig. 6 and obtained on corroded coins, clearly demonstrate this similarity.

Because corrosion can produce the same effects on the surface of the silver–copper alloys as segre-

Table 4
Techniques used for the data reported in Fig. 6

Reference	[15]	[13]	[21]	[26]	[27]	[17]	[16]	This study
Method for the surface analysis	XRF–WDS	PIXE 2 MeV protons SRXRF	PIXE external beam, 2.8 MeV	XRF–EDS on surface	PIXE external proton beam, 2.57 MeV on the sample	PIXE 1.4 MeV protons on surface	EDXRF on surface	PIXE & SEM–EDS on surface
Method for the core analysis	Walker's data [1] XRF–EDS on abraded edges	NAA	Expected concentration	XRF–EDS after abrasion	PIXE external beam, 2.57 MeV protons after mechanical abrasion – official fineness	PIXE 1.4 MeV protons. Profile on the cross-section	SEM–EDX on cross-section	PIXE & SEM–EDS on cross-section

PIXE: particle induced X-ray emission; SEM–EDS: scanning electron microscope with energy-dispersive X-ray microanalysis (or spectrometry); SRXRF: synchrotron X-ray fluorescence; EDXRF or XRFA–EDS or XRF–EDS: energy-dispersive X-ray fluorescence or X-ray fluorescence (analysis) with energy-dispersive spectrometry; XRF–WDS: X-ray fluorescence analysis with wavelength-dispersive spectrometry; NAA: thermal neutron analysis.

gation during fabrication does, it seems difficult to determine the weight of each contribution for ancient coins. However, we have demonstrated that direct surface enrichment can be achieved during the fabrication of the blank. This direct handling has the advantage of saving time because the hammering is no longer necessary to laterally distribute the silver-rich phase to the surface of the blank. This advantage must have been known and used by the Romans.

5. Conclusion

The fabrication of replications of silver–copper alloy coin blanks has demonstrated the possibility of direct production of an external surface enriched in silver. This process, which is referred to in this study as ''direct enrichment'', makes it possible to obtain layers of several tens of micrometers in thickness. It has been possible to determine three types of enrichment, depending on the initial composition of the alloy.

The comparison of replications with the results of analyses performed on ancient coins, suggests that this type of enrichment was employed by coin minters in ancient times. Additional studies will be necessary in order to more finely distinguish the effects of human intervention from long-term corrosion processes.

However, whatever the origin of the enrichment, the enriched layer plays a decisive role in the analysis results when these are obtained using conventional X-ray spectrometry methods. If the thickness of enriched layers is greater than the depth under study, only the composition of this layer is accessible. Nevertheless, in this case, a classification of the coins in three groups of core compositions (Ag > 72%, 20 < Ag < 72% or Ag < 20%) may be attempted. This procedure is only possible when coins have not been subjected to blanching or excessive cleaning. Generally, and to be realistic, this study confirms that, unfortunately, non-destructive surface analysis methods may not be directly applied in the determination of the fineness of ancient silver–copper coins.

Acknowledgments

L. Beck would like to thank R. Klockenkämper for providing the digital files of the data presented in Fig. 6. FNAA were performed at the Centre E. Babelon by using the cyclotron of the CERI laboratory (CNRS – Orléans). The authors acknowledge J.-N. Barrandon, M. Blet-Lemarquand and A. Deraisme for the FNAA experiment. The authors are grateful to the anonymous referees for their useful comments.

References

[1] D.R. Walker, Brit. Archaeol. Rep. Suppl. Ser. 5, 22 and 40, Oxford, 1976–1978.
[2] C.E. King, J.P. Northover, in: H. von Kaenel (Ed.), Der Münzhort aus dem Gutshof in Neftenbach, Zürich Denkmalpflege Archäologische Monographien, Vol. 16, 1993, p. 110.
[3] R. Cesareo, G.E. Gigante, A. Castellano, M.A. Rosales, M. Aliphat, F. de La Fuente, J.J. Meitin, A. Mendoza, J.S. Iwanczyk, J. Pantazis, J. Trace Microprobe Tech. 14 (1996) 711.
[4] M.F. Guerra, X-Ray Spectrom. 27 (1998) 731.
[5] G. Harbottle, Radiochemistry 3 (1977) 33.
[6] F. Beauchesne, J.-N. Barrandon, Revue d'Archéométrie 10 (1986) 75.
[7] P. Meyers, Archaeometry 11 (1969) 67.
[8] J.-N. Barrandon, J. Radioanal. Chem. 55 (1980) 317.
[9] F. Beauchesne, J.-N. Barrandon, L. Alves, F.B. Gil, M.F. Guerra, Archaeometry 30 (1988) 187.
[10] L.H. Cope, in: E.T. Hall, D.M. Metcalf (Eds.), Methods of Chemical and Metallurgical Investigation of Ancient Coinage, RNS Special Publication No. 8, 1972, p. 261.
[11] S. La Niece, in: S. La Niece, P. Craddock (Eds.), Metal, Plating and Platination, Butterworth–Heinemann, London, 1993, p. 201.
[12] M. Basutçu, Ph.D. Thesis, Université Paris VI, 1980.
[13] I. Brissaud, P. Chevallier, C. Dardenne, N. Deschamps, J.P. Frontier, K. Gruel, A. Taccoen, A. Tarrats, J.X. Wang, Nucl. Instr. and Meth. B 49 (1990) 305.
[14] G. Weber, J. Guillaume, D. Strivay, H.P. Garnir, A. Marchal, L. Martinot, Nucl. Instr. and Meth. B 161–163 (2000) 724.
[15] R. Klockenkämper, H. Bubert, K. Hasler, Archaeometry 41 (1999) 311.
[16] R. Linke, M. Schreiner, G. Demortier, M. Alram, X-Ray Spectrom. 32 (2003) 373.
[17] Z. Smit, P. Kos, Nucl. Instr. and Meth. B 3 (1984) 416.
[18] R. Linke, M. Schreiner, Mikrochim. Acta 133 (2000) 165.

[19] M. Bompaire, F. Dumas, in: Turnhout (Ed.), Numismatique médiévale, monnaies et documents d'origine française, 2000.
[20] H. Gitler, M. Ponting, Glaux 16, Edizioni ennerre, Milano, 2003.
[21] A.-M. Meyer, G. Demortier, Nucl. Instr. and Meth. B 49 (1990) 300.
[22] E.T. Hall, Archaeometry 4 (1961) 62.
[23] G.F. Carter, Archaeometry 19 (1977) 67.
[24] F. Pilon, Trésors Monétaires XVII (1998) 77.
[25] L. Beck, S. Reveillon, S. Bosonnet, D. Eliot, F. Pilon, in: Proceedings of the 33rd International Symposium on Archaeometry, April 2002, Amsterdam, Geoarchaeol. Bioarchaeol. Studies, submitted for publication.
[26] J. Tate, Nucl. Instr. and Meth. B 14 (1986) 20.
[27] D. Strivay, Nouvelles applications des techniques d'analyse par faisceau d'ions, Ph.D. Thesis, Université de Liège, Belgique, 2001.